

## Relaxation Time of a Chiral Quantum $R$ - $L$ Circuit

J. Gabelli,<sup>1</sup> G. Fève,<sup>1</sup> T. Kontos,<sup>1</sup> J.-M. Berroir,<sup>1</sup> B. Placais,<sup>1,\*</sup> D. C. Glattli,<sup>1,2</sup> B. Etienne,<sup>3</sup> Y. Jin,<sup>3</sup> and M. Büttiker<sup>4</sup>

<sup>1</sup>Laboratoire Pierre Aigrain, Département de Physique de l'Ecole Normale Supérieure, 24 rue Lhomond, 75005 Paris, France

<sup>2</sup>Service de Physique de l'Etat Condensé, CEA Saclay, F-91191 Gif-sur-Yvette, France

<sup>3</sup>Laboratoire de Photonique et Nanostructures, CNRS, route de Nozay, F-91460 Marcoussis, France

<sup>4</sup>Université de Genève, 24 Quai Ernest Ansermet, CH-1211 Genève, Switzerland

(Received 26 January 2007; published 20 April 2007)

We report on the GHz complex admittance of a chiral one-dimensional ballistic conductor formed by edge states in the quantum Hall regime. The circuit consists of a wide Hall bar (the inductor  $L$ ) in series with a tunable resistor ( $R$ ) formed by a quantum point contact. Electron interactions between edges are screened by a pair of side gates. Conductance steps are observed on both real and imaginary parts of the admittance. Remarkably, the phase of the admittance is transmission independent. This shows that the relaxation time of a chiral  $R$ - $L$  circuit is resistance independent. A current and charge conserving scattering theory is presented that accounts for this observation with a relaxation time given by the electronic transit time in the circuit.

DOI: 10.1103/PhysRevLett.98.166806

PACS numbers: 73.23.Ad, 73.43.Cd, 73.43.Fj, 73.63.-b

Violation of classical electrokinetic laws is a hallmark of quantum transport. In the dc regime, it is well known that transport is nonlocal over the electronic coherence length. This leads to the nonadditivity of parallel conductances [1] and to quantum composition laws to relate impurity scattering to resistance. Recently a similar manifestation of quantum coherence has been reported by Gabelli *et al.* [2,3] in the ac regime where the resistance which determines the  $RC$ -charge relaxation time of a mesoscopic capacitor is found to be quantized at half of a resistance quantum. This observation, in agreement with predictions of Büttiker, Thomas, and Prêtre [4,5], establishes the concept of a charge relaxation resistance [6] different from the standard dc Landauer resistance. A second fundamental dynamical time scale is the  $L/R$  time of a mesoscopic circuit which in macroscopic conductors is determined by the ratio of the inductance and the resistance of the sample.

Here we investigate a series combination of an inductive and resistive element and demonstrate that macroscopic kinetics does not account for the correct ac response. In this case, chirality is responsible for the observed nonclassical behavior. The inductive conductor is made of the kinetic inductance of electrons in edge states [7–9] of a 2D electron gas (2DEG) quantum Hall bar [10]. The resistive element is a quantum point contact (QPC) [11]. Theory [12] predicts that edge channels that connect two reservoirs contribute to the impedance inductively due to kinetic effects, whereas reflected edge channels contribute capacitively. Importantly, in the present setup, the interedge coupling is reduced due to the large bar width and further minimized by using side gates strongly coupled to the edge states. Our main result is that the relaxation time of the quantum  $R$ - $L$  circuit is not the classical  $L/R$  time but the electronic transit time of the circuit.

In our work the sample is still short compared to the wavelength of an edge magnetoplasmon. Previous experimental investigations of the electromagnetic response of

Hall bars [13–16] have addressed the regime where the response is well accounted for by collective excitations called edge magnetoplasmons [17] with wavelength short compared to the dimensions of the sample. References [13,15] have extensively studied the time domain and Ref. [16] the frequency domain.

In this Letter we report on phase-resolved impedance measurements of a quantum  $R$ - $L$  circuit in the edge state regime at GHz frequency and milliKelvin temperatures. With increasing QPC transmission, dc-like conductance steps are observed on both quadratures of the admittance. Remarkably, the admittance phase is independent of the number of transmitted modes and of their transmission. This shows that the relaxation time of the chiral  $R$ - $L$  circuit is resistance independent. A current and charge conserving scattering theory extending Ref. [12] is presented that accounts for this observation with a relaxation time given by the electronic dwell time in the circuit.

The sample is a 50  $\mu\text{m}$  long and 6  $\mu\text{m}$  wide Hall bar made in a GaAs/AlGaAs electron gas of nominal density  $n_s = 1.3 \times 10^{11} \text{ cm}^{-2}$  and mobility  $\mu = 3 \times 10^6 \text{ cm}^2 \text{ V}^{-1} \text{ s}^{-1}$ . A magnetic field of  $B = 0.224 \text{ T}$  and  $B = 0.385 \text{ T}$  is applied in the spin degenerate quantum Hall regime (filling factors  $N = 24$  and  $N = 14$ , respectively) so that edge states are well developed. The bar is interrupted in its middle by a pair of quantum point contacts (inset of Fig. 1). Only the first QPC is active with a negative voltage bias ( $V_g \sim -1 \text{ V}$ ). Electron gas being fully depleted beneath it, the gate to 2DEG capacitance is small. The grounded gate of the second QPC widely overlaps the electron gas. This results in a large gate 2DEG capacitance  $c_g \sim 30 \text{ fF}$  (for a gate length  $l_g \sim 10 \mu\text{m}$ ) which efficiently screens the interedge interactions. We estimate  $c_g \gg c_H$ , with  $c_H \sim 1 \text{ fF}$  the edge-to-edge capacitance for the full Hall bar length. Long and wide non-dissipative leads (not shown in Fig. 1) connect the sample to the contact pads.

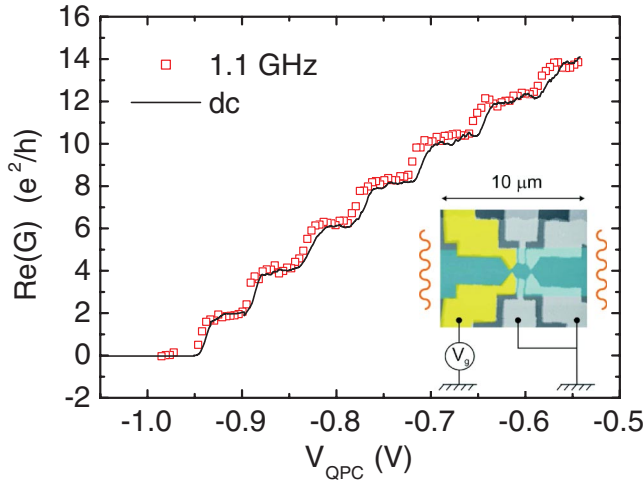


FIG. 1 (color). Quantized steps in the dc conductance and rf transmission of the circuit as a function of the QPC gate voltage. The solid line has been shifted by +10 mV along the voltage axis to avoid curve overlapping which otherwise obscures figure clarity. Temperature and magnetic field are, respectively, 50 mK and 0.224 T.

The sample is mounted between two impedance-matched  $50 \Omega$  coplanar lines. Its impedance being large ( $\geq 10 \text{ k}\Omega$ ), the rf conductance  $G(\omega)$  is simply proportional to the rf transmission of the setup. Phase is calibrated by assigning a purely capacitive admittance ( $\approx 40 \text{ fF}$ ) to the sample at the pinchoff. This is corroborated by the vanishing of the dc conductance.

Figure 1 shows the real part  $\text{Re}(G)$  at the opening of the QPC. The large filling factor in the Hall bar ( $N = 24$ ) allows the QPC to control the transmission of a large number of edge states. As can be seen in the figure, the rf data are proportional to the dc one. In the following we shall assign the value  $2e^2/h$  to the  $\text{Re}(G)$  steps as a calibration of our setup.

Figure 2 shows  $\text{Re}(G)$  and  $\text{Im}(G)$  at  $N = 14$  for the opening of the first three channels. Note that  $\text{Im}(G) < 0$  denotes an inductive contribution.  $\text{Re}(G)$  and  $\text{Im}(G)$  show similar regular steps as a function of QPC transmission. The inductance step amplitude is  $\approx 1 \mu\text{H}$ . In fact both quadratures are mutually proportional, as can be seen in the Nyquist plot of Fig. 3. This corresponds to a transmission-independent phase factor,  $\tan(\varphi) = -\omega\tau = \text{Im}(G)/\text{Re}(G)$ . It is well explained by a constant relaxation time  $\tau$ , in strong contrast with the time constant ( $L/R \propto \text{Re}(G)$ ) of a classical circuit. As additional information, the inset of Fig. 3 depicts the linear magnetic field dependence of  $\tau$ . These are the main results of our experiment. We propose below an interpretation relying on the theory developed by Christen and one of us [12] for the low frequency admittance of chiral conductors.

In Ref. [12] the emittance  $E = \text{Im}(G/\omega)$  has been calculated for the case of a Hall bar with fully transmitted and/or fully reflected edge states. The calculation takes into

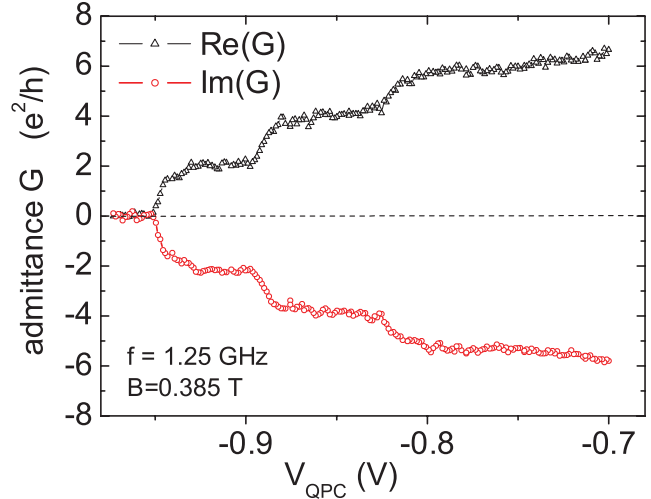


FIG. 2 (color). Real and imaginary parts of the rf admittance of the quantum Hall conductor as a function of the QPC voltage at  $T = 50 \text{ mK}$ . Both signals show steps at the opening of the first conducting channel. The negative imaginary part corresponds to a negative emittance which is characteristic of an inductive behavior.

account both interedge coupling and coupling to side gates. Here we consider the case of a quantum Hall bar coupled to side gates in series with a quantum point contact which controls the number of transmitted channels and their transmission [see Fig. 4(a)]. Let  $N$  be the number of filled Landau levels (for simplicity we do not take into account spin degeneracy in the calculations),  $n$  be the number of

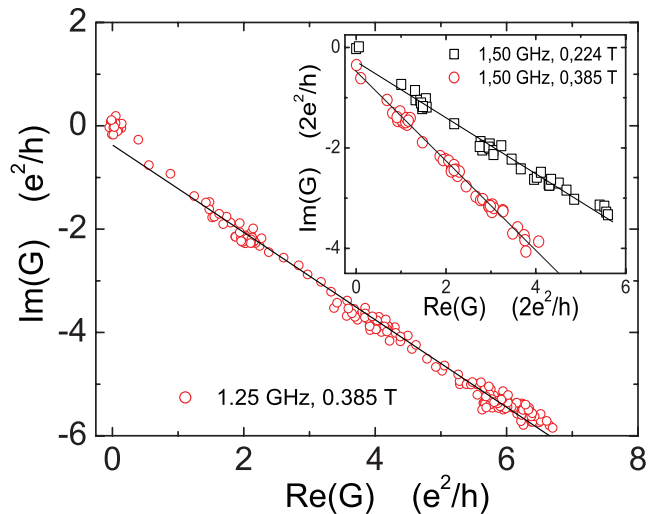


FIG. 3 (color). Main frame: Nyquist representation of the data of Fig. 2 showing that the admittance phase is constant as a function of the number of transmitted channels and of their transmission. Point accumulation corresponds to the admittance plateaus in Fig. 2. Inset: similar measurements obtained at two different magnetic fields showing the linear increase of the admittance phase with magnetic field.

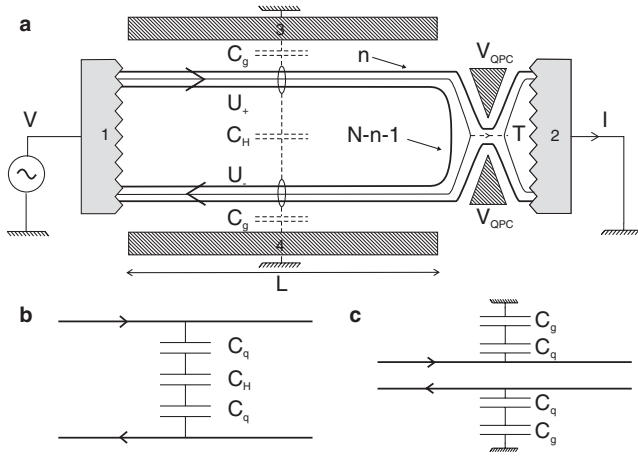


FIG. 4. (a) Schematics of a quantum Hall bar with  $N$  edge states in series with a quantum point contact (QPC) with  $n$  fully transmitted channels and one partially transmitted channel. Electrochemical equivalent circuit of a Hall bar in the limit of weak edge to gate coupling (b) and weak interedge coupling (c). Notations are specified in the text.

fully transmitted modes, and  $T$  the transmission of the partially transmitted one so that  $(N-n-1)$  modes are totally reflected. The length gate  $l_g$  is small enough that propagation effects can be neglected. Thus charging of edge states is uniform but might differ on the upper and lower branch of the edge state. Thus we can assume that the edge states on the left upper side (labeled  $+$ ) of the sample experience the same electrostatic potential  $U+$  and all the edge states on the left lower side (labeled  $-$ ) experience the potential  $U-$ . The upper and lower edge states on the left side are equally coupled to side gates with capacitance  $c_g$  and the long range electrostatic interactions between the upper and lower edges are described by a capacitance  $c_H$  [see Fig. 1(b)]. For simplicity, we take all left edge states to have the same density of states,  $\nu = l_g/hv_D$ , where  $v_D$  is the drift velocity.  $v_D$  is the ratio of the confining electric field to the applied magnetic field and is, therefore,  $\propto N$ . The quantum capacitance per channel is given by  $c_q = e^2\nu = l_g e^2/hv_D$ .

The low frequency response of the conductor is of the form  $dI_\alpha(\omega)/dV_\beta(\omega) = G_{\alpha\beta} - i\omega E_{\alpha\beta} + \dots$ , where  $\alpha, \beta$  label current contact indices 1 and 2 and gate indices 3 and 4 [18].  $G_{\alpha\beta} \neq 0$  only for current contacts.  $E_{\alpha\beta}$  is a four terminal emittance matrix for the quantum conductor with its gates. According to Ref. [12], the emittance is

$$E_{\alpha\beta} = e^2 \sum_{k=+,-} \left[ \frac{dN_{\alpha k\beta}}{dE} - \frac{dN_{\alpha k}}{dE} u_{k,\beta} \right], \quad (1)$$

where  $dN_{\alpha k\beta}/dE$  is the partial density of states of carriers injected in contact  $\beta$  that reach the upper edge  $k = +$  (or the lower edge  $k = -$ ), and exit the sample through contact  $\alpha$ .  $dN_{\alpha k}/dE = \sum_\beta (dN_{\alpha k\beta}/dE)$  is the emissivity of region  $k = \pm$  irrespective of the contact from which the

carriers are incident. The characteristic potential  $u_{k,\beta}$  relates the change of the electrostatic potential of conductor  $k$  to that of the electrochemical potential of contact  $\beta$ . In our geometry the only nonzero partial density of states are

$$\begin{aligned} \frac{dN_{1,\pm,1}}{dE} &= [(1-T) + N - (n+1)]\nu, \\ \frac{dN_{2,+1}}{dE} &= \frac{dN_{1,-,2}}{dE} = (T+n)\nu, \end{aligned}$$

from which we find the emissivities  $dN_{\alpha k}/dE$ . We next need to find the characteristic potentials  $u_{k,\beta}$  on the upper and lower edges of the conductor  $k = \pm$  for each of the four contacts  $\beta = 1, 2, 3, 4$ . To this end we follow closely Ref. [12] and find the emittance matrix. The two-terminal admittance measurement considered in this work is determined by the matrix element [19]  $E_{2,1} \equiv E$ . We find

$$E = -c_{\mu g} \frac{(T+n)}{N} - \eta c_{\mu H} \frac{(T+n)^2}{N^2}, \quad (2)$$

where

$$c_{\mu g} = \frac{Nc_q c_g}{c_g + Nc_q}, \quad c_{\mu H} = \frac{Nc_q c_H}{2c_H + Nc_q}, \quad (3)$$

$$\eta = \frac{1}{1 + c_g/Nc_q} \frac{1}{1 + c_g/(2c_H + Nc_q)} \quad (4)$$

are, respectively, the electrochemical capacitance between one edge and its side gate and the mutual capacitance of the edge states across the Hall bar. The coefficient  $\eta < 1$  vanishes for strong gate coupling ( $c_g \gg c_q$ ). Note that  $v_D \propto N$ , so that  $N\nu$ ,  $c_{\mu H}$ , and  $c_{\mu g}$  do not depend on  $N$ .

For our experiment where interedge coupling is weak ( $c_H \ll c_q \leq c_g$ ),  $E \simeq -c_{\mu g}(T+n)/N$ , we obtain

$$G(\omega) = G_0 \left( 1 - i\omega \frac{h}{e^2} \frac{c_{\mu g}}{N} \right), \quad (5)$$

where  $G_0 = (n+T)e^2/h$  is the Landauer dc conductance. Remarkably  $G(\omega)$  exhibits a transmission-independent phase in agreement with the experiment. Here the negative bar emittance can be interpreted with the equivalent circuit in Fig. 4(c) in terms of leakage currents to the gate. It can be shown that the classical addition of the Hall bar and the QPC impedances gives a different result with a transmission-dependent phase factor. This corresponds to the situation where a fictitious reservoir is inserted between the two components which amounts essentially to break the chirality of the experiment. We thus observe a violation of classical laws which is here a pure effect of chirality. The phase factor is given by the transit time of electrons through the Hall bar  $\tau = l_g/\tilde{v}_D$ , where  $\tilde{v}_D = v_D + (e^2 N l_g / hc_g)$  is the drift velocity which takes into account the screening by the side gate. Note that  $\tilde{v}_D \propto N$  is in-

versely proportional to the magnetic field. This magnetic field dependence is clearly observed in the experiment (inset of Fig. 3). From the slope ( $\approx -0.89$ ) of the Nyquist diagram obtained at  $B = 0.385$  T (main frame), and  $l_g \sim 10 \mu\text{m}$ , we estimate a drift velocity of  $\tilde{v}_D \sim 10^5$  m/s in order of magnitude agreement with the numbers in the literature [15].

We consider now the opposite case of a nonchiral quantum wire (i.e., a carbon nanotube) with strong interedge coupling ( $c_g \ll c_q \lesssim c_H$ ). We obtain

$$G(\omega) = G_0 \left( 1 - i\omega G_0 \frac{\hbar^2}{e^4} c_{\mu H} \right). \quad (6)$$

It corresponds to the lowest order development for the admittance of the Landauer resistance  $1/G_0$  in series with the Hall-bar electrochemical inductance  $L_\mu = (\hbar^2/e^4)c_{\mu H}/N^2$ . In this nonchiral situation classical laws are recovered. The negative Hall-bar emittance can be interpreted with the equivalent circuit in Fig. 4(b), in terms of displacement countercurrents proportional to frequency. For very strong interedge coupling ( $c_H \rightarrow \infty$ ),  $L_\mu$  reduces to the usual kinetic inductance of a quantum wire,  $L_{\text{kin}} = (\hbar^2/e^2)(\nu/2N)$  [20,21]. The signature of this regime would be a linear variation of the admittance phase (i.e.,  $\tau$ ) with transmission, which corresponds to a circle arch in the Nyquist diagram.

In conclusion, we have provided phase-resolved measurements of the admittance of a quantum Hall bar coupled to gates in series with a quantum point contact. This realizes the simplest chiral quantum  $R$ - $L$  circuit. We observe quantized steps in both the active and reactive parts of the admittance with a remarkable transmission-independent phase. The phase is directly related to the transit time of the electrons in the Hall bar. This interpretation is further supported by the expected magnetic field dependence of the transit time. Our measurements are well described by a scattering theory in the limit of strong side-gate coupling, allowing for a direct determination of the electronic transit time. Our work demonstrates that interesting novel transport quantities such as the mesoscopic analogs of the  $RC$  and  $L/R$  times become accessible in the GHz range provided the measurement is carried out on a sample with properties that can be tuned over a wide range, for instance, as here with a QPC.

The Laboratoire Pierre Aigrain (LPA) is the CNRS-ENS No. UMR8551 associated with Universities Paris 6 and Paris 7. The research has been supported by No. ANR-05-NANO-028. The work of M. B. was supported by the LPA, the Swiss NSF, and the STREP project SUBTLE.

\*Electronic address: Bernard.Placais@lpa.ens.fr

- [1] R. A. Webb, S. Washburn, C. P. Umbach, and R. B. Laibowitz, Phys. Rev. Lett. **54**, 2696 (1985).
- [2] J. Gabelli, G. Fève, J.-M. Berroir, B. Placais, A. Cavanna, B. Etienne, Y. Jin, and D. C. Glatli, Science **313**, 499 (2006).
- [3] For additional experimental results, see J. Gabelli, Ph.D. thesis, Ecole Normale Supérieure, Paris 2005, <http://tel.archives-ouvertes.fr/tel-00011619>.
- [4] M. Büttiker, H. Thomas, and A. Prêtre, Phys. Lett. A **180**, 364 (1993); M. Büttiker, A. Prêtre, and H. Thomas, Phys. Rev. Lett. **70**, 4114 (1993).
- [5] A. Prêtre, H. Thomas, and M. Büttiker, Phys. Rev. B **54**, 8130 (1996).
- [6] The experiment Ref. [2] reports on the high magnetic field response using spin polarized edge channels. A recent theoretical discussion of the low field case is S. Nigg, R. Lopez, and M. Büttiker, Phys. Rev. Lett. **97**, 206804 (2006); J. Wang, B. Wang, and H. Guo, cond-mat/0701360 [Phys. Rev. B (to be published)].
- [7] B. I. Halperin, Phys. Rev. B **25**, 2185 (1982).
- [8] M. Büttiker, Phys. Rev. B **38**, 9375 (1988).
- [9] D. B. Chklovskii, B. I. Shklovskii, and L. I. Glazman, Phys. Rev. B **46**, 4026 (1992).
- [10] K. v. Klitzing, G. Dorda, and M. Pepper, Phys. Rev. Lett. **45**, 494 (1980).
- [11] B. J. van Wees, H. van Houten, C. W. J. Beenakker, J. G. Williamson, L. P. Kouwenhoven, D. van der Marel, and C. T. Foxon, Phys. Rev. Lett. **60**, 848 (1988); D. A. Wharam, T. J. Thornton, R. Newbury, M. Pepper, H. Ahmed, J. E. F. Frost, D. G. Hasko, D. C. Peacock, D. A. Ritchie, and G. A. C. Jones, J. Phys. C **21**, L209 (1988).
- [12] T. Christen and M. Büttiker, Phys. Rev. B **53**, 2064 (1996).
- [13] R. C. Ashoori, H. L. Stormer, L. N. Pfeiffer, K. W. Baldwin, and K. West, Phys. Rev. B **45**, 3894 (1992).
- [14] V. I. Talyanskii, J. E. F. Frost, M. Pepper, D. A. Ritchie, M. Grimshaw, and G. A. C. Jones, J. Phys. Condens. Matter **5**, 7643 (1993).
- [15] G. Sukhodub, F. Hohls, and R. J. Haug, Phys. Rev. Lett. **93**, 196801 (2004).
- [16] R. H. Blick, R. J. Haug, D. W. van der Welde, K. von Klitzing, and K. Eberl, Appl. Phys. Lett. **67**, 3924 (1995).
- [17] D. C. Glatli, E. Y. Andrei, G. Deville, J. Poitrenaud, and F. I. B. Williams, Phys. Rev. Lett. **54**, 1710 (1985).
- [18] To map the dynamics onto  $L$ - $R$  circuit elements considered in this work a first order expansion is sufficient.
- [19] The magnetic field symmetry of the emittance matrix is investigated in W. Chen, T. P. Smith, M. Büttiker, and M. Shayegan, Phys. Rev. Lett. **73**, 146 (1994).
- [20] P. J. Burke, I. B. Spielman, J. P. Eisenstein, L. N. Pfeiffer, and K. W. West, Appl. Phys. Lett. **76**, 745 (2000).
- [21] P. J. Burke, IEEE Trans. Nanotechnol. **1**, 129 (2002).